Iranian Journal of Chemical Engineering
Vol. 15, No. 1 (Winter 2018), IAChE

Investigation of Spent Caustic Wastewater Treatment through Response Surface Methodology and Artificial Neural Network in a Photocatalytic Reactor

A. Ahmadpour [1], A. Haghighi Asl [1*], N. Fallah [2]

[1] Faculty of Chemical, Gas and Petroleum Engineering, Semnan University, Semnan, Iran
[2] Chemical Engineering Department, Amirkabir University of Technology, Tehran, Iran

ARTICLE INFO

Article history:
Received: 2017-02-01
Accepted: 2017-03-13

Keywords:
ANN
RSM
COD
ZnO
Photocatalytic Removal

ABSTRACT

In this research, photocatalytic degradation method was introduced to clean up Spent Caustic of Olefin units of petrochemical industries (neutralized Spent Caustic by means of sulfuric acid). In the next step, an adaptable method and effective parameters in the process performance were investigated. Chemical oxygen demand (COD) was measured by the commercial zinc oxide synthesized with precipitation synthesis method in a two-shell photoreactor. The percent of reduction of COD in the photocatalytic process was modelled using a Box–Behnken design and artificial neural network techniques. It was concluded that the ANN was a more accurate method than the design of experiment was. The effect of important parameters including oxidant dosage, aeration rate, pH, and catalyst loading was investigated. The results showed that all of the parameters, except pH, had positive effects on increasing COD removal. According to the obtained results, adsorption and photolysis phenomena had a negligible effect on COD removal.

1. Introduction

Nowadays, resultant progresses in different fields and technologies and their application in industry lead to the appearance and increase of pollutants and hazardous materials which can resist against biological decomposition. Requisiteness of environment protection is an indubitable principle nowadays, which has been communalized, and this necessity has been increasingly of high concern due to development of industries and technologies eventuating in contamination. Of course, without environmental changes, industrial and economical growth cannot be expected. In addition, environmental experts are not after such an impossible affair. However, this reality makes it explicit that giving up the search for stable development principles and environmental protection can blind us from imagining a desirable future for the present and next generations. Industrial pollutions apply reduplicated pressure to the ecosystems and, as a consequence, to the biological

[*] Corresponding author: ahaghighi@semnan.ac.ir

diversity; without taking urgent measures, this irreversible proceeding would leave us with a biologically poor world for the next generations. Industrial wastewater has different chemical/physical specifications relative to urban wastewater due to broadness of initial consumption materials, products, and manufacture processes. As a consequence, lack of treatment of this wastewater before excreting to the environment poduces numerous biological problems. Among these compounds, hazardous compounds mainly from petrochemical complexes and many other industrial and chemical units are excreted and left into the environment without any proper treatment, or regard for biological perils. Again, with respect to the increase of limitations emanating from new and fastidiously environmental biology rules to preserve equivalence of natural ecosystem, efficient treatment methods are required to remove these materials or, at least, transform them to minor molecules to facilitate their clean-up process. Existing pollutants of petrochemical wastewater are considered as the most substantial ones whose removal is always important due to obtaining the environmental biology standards and waste water control. Since direct biological treatment of some specific wastewater of this industry is not possible, modern methods are proposed such as advanced oxidant processes. These methods are based on producing very active species that are able to oxidize a vast range of organic pollutants. Among the advanced oxidant processes, heterogeneous photocatalysts produce satisfactory results of degradation of toxic and resistant organic materials and, then, produce materials with lower toxicity and wih biological decomposition capability.

Photocatalysts, including TiO_2, ZNO, WO_3, etc., have been investigated so far, whose titanium dioxide has been extensively used for removing a large amount of organic compounds because of high photocatalytic activity, non-toxicity, chemical stability, and cost-effective among these nano-photocatalysts. On the other hand, heterogeneous photocatalysts used in the several forms, low quantum efficiency relative to visible light, photoreactor design, recovery and secondary usage of catalyst, production of toxic intermediates, and problems related to catalyst inactivity are defects of this method; the application of this method is justifiable when defects are eliminated. With respect to costs and hazards of ultraviolet light, it is necessary to obtain a catalyst able to be active in the visible light or even solar light for using a photocatalytic method at industrial scale and wastewater treatment. Perception of effect of various factors on the photocatalytic process efficiency in the design of this process is of highest importance for treatment on the industrial scale [1].

At the Olefin units of petrochemical industries, as a consequence of sulfuric hydrogen removal, toxic and harmful compound of sodium sulfide is deteced in the outlet wastewater. Used Caustic is known as harmful wastewater due to high acidity, sulfide and hydrocarbon compounds, residual free sodium hydroxide, and organic salts. Caustic sodium hydroxide flow with respect to used ones as wastewater should be cleaned up, because high concentration of sulfide makes micro-organisms toxicant. In this research, since produced Spent Caustic wastewater contains a vast range of hydrocarbons, selection of photocatalytic oxidations method for initial degradation of

pollutants before biologic treatment and after physical pre-treatment can be rational and effective. Moreover, sulfide pollution, including hydrogen sulfide, is toxic and very corrosive which damages the equipment, and if produced wastewater contains those pollutants, production of insoluble metallic sediments is one of problems that takes place. Using a photocatalytic oxidation method with the oxidant material, including oxygen and or hydrogen peroxide, can oxidize sulfide and hydrocarbon compounds and reduce it enough to distinctive standards. Reports indicate that photocatalytic degradation of these compounds depends on the type and composition of the catalyst, light intensity, initial material concentration, amount of catalyst, reaction solution pH, catalyst utilizition method, and calcination temperature. Perception of effect of various factors on the photocatalytic process efficiency in the design of this process is of highest importance for treatment on the industrial scale. Spent Caustics contain types of sulfide, cresyle, and naphthen. Sulfide-type caustics occur when light oil cuts are used in order to transform CO_2 and H_2S into salty state by means of Caustic solution. Cresylic type is obtained during cracking process, and phenol and creysul are the main harmful materials. Naphthenic type also contains high concentration of multi-ring aliphatic organic compounds. The most outdated spent caustic wastewater treatment is wet air oxidation (WAO) process which is in fact oxidation with liquid phase by means of oxygen or air. This method has three different operating conditions. In the low temperature operating condition, oxidation process is done at temperature 200 ºC and pressure 27.5 barg. This process has a relative ability of transforming sulfide into sulfate and thiosulfate. In the medium temperature operating condition, which is mainly used for cleaning up spent caustic of naphthenic type, oxidation process is done at 200-260 ºC and 25.5- 86 barg, and sulfide is degraded to oxidized sulfate and mercaptan. In the high temperature operating condition, which is mainly used for cleaning up spent caustic of cresylic type, oxidation process is done at 240-260 ºC and 55-85 barg where complete sulfide, mercaptan and cresylic acids oxidation operation take place [2]. Spent caustic wastewater, due to specific conditions, including large amount of TDS, sulfide, COD, and pH (more than 12) and different amounts of phenol, particularly has attracted researchers' attention, and many people in the foreign countries have been studied and published using different methods, including syncretist methods of neutralization and devesting, and also different advanced oxidation methods (fenton, ozonation, wet air oxidation, and photo-oxidation processes).

Mara et al. (2000) investigated the caustic wastewater treatment using a wet air oxidation method. They reduced COD level from 72000 to 15000 miligrams per liter by employing caustic wastewater and, then, diluting with water at 260 ºC and pressure 90 barg. They stressed the necessity of outlet wastewater cooling, diluting and lack of ability of this process in order to achieve environmental biology evacuation standards and high costs [3]. According to other studies, Hsiungsheu et al. study in 2001 managed to remove more than 94 percent of COD from wastewater by using a syncretist process of neutralization - devesting – fenton. His study showed that neutralization – devesting compound is able to reduce COD from 40000

miligrams per liter and sulfide from 19000 miligrams per liter to 1400 miligrams per liter [4]. Rodriguez et al. in 2008 reported their study on the treatment of caustic wastewater by using electrofenton. He reported 95 percent removal of COD with pH value of 4 and temperature 40 ºC and application of 100 miligrams per liter of iron [5]. Nueza et al. in 2009 reported caustic wastewater treatment using the electrochemical process. He reported 93 percent removal of COD [6]. YuZZ et al. in 2004 reported caustic wastewater treatment using syncretist UV/H_2O_2 $/O_3$ process. Also, UV/H_2O_2 $/O_3$ process is able to remove 44 percent of COD [7]. Hawari et al. in 2015 investigated caustic wastewater treatment. They reported 98 percent removal of COD and 99 percent removal of sulfide at pH value of 1.5. Also, it is reported that oxidation by means of H_2O_2 is able to remove 89 percent of COD at pH value of 2.5 and consumption of 19 milimolar per liter of hydrogen peroxide [8]. Abdulah et al. in 2011 investigated synthesized spent caustic wastewater treatment using photofenton oxidation. They used response surface method for experiment design of this research [9]. Chen chen et al. in 2012 investigated the actual spent caustic wastewater treatment with COD amount of 25000 using catalytic and usual wet air oxidation methods and COD reduced amount of 75 and 95 percent reported by using usual and catalyitic methods, respectively [10]. Alaiezadeh in 2012 investigated COD reduction of spent caustic of south pars gas refinery by using electrical coagulation mechanism. Maximum efficiency of this process (91 percent) during 105 min effective time, diluting by ratio of 2 and 1 voluminosity of wastewater and water, respectively, with TDS=40000 ppm, acidity of 9, flow density of 62.8 miliAmper per square centimiter and 1.32 g/lit of $FeSO_4$ [11]. Selection of an experiment design is based on purposes and number of factors. In the photocatalytic systems, several parameters, such as temperature, PH, catalyst amount, etc., influence efficiency of photocatalytic degradation process. Usually, existence of several factors in photocatalytic reactions leads to do more experiments, large expenses, and long times. So, for the purpose of persuing these factors in the process efficiency, experiments are carried out in a regular form, obtained data arranged, and the number of experiments reduced; if possible, a set of these series leads to the optimization of design. Thereby, using design of experiments will be a suitable choice. Design of experiment methods is significantly important gadgets for modifying performance of generative processes, optimizing and developing of new processes which cause timesaving and efficient economy. For problems in which there is no exact relationship between inlets and outlets, response surface methods (RSM) are proper superseded ones. These methods are determinated using estimative-approximate functions of design space based on designed models obtained from design of experiment. Response surface method purpose is response optimization and also interpolation of unknown experiment points and true approximate from a probable response of that points. Among the response surface methods, two well-known designs titled as central composite design (CCD) and Box-Behnken can be mentioned. Two researchers, Box and Behnken, proposed another type of three surface designs in 1960. Resultant designs are efficient due to ingredients. A significant point in the Box/Behnken method is that the

geometric form of this design relative to CCD method contains no point at the cubic corners, wherein cubic corner points show the combinations of variable surfaces whose examination is impossible or economically non-costeffective due to physical restrictions, which can be considered as the advantage of this design[12].

Artificial neural networks (ANNs) and response surface methodology (RSM) are important approaches in the field of chemical reactions for process modelling and optimization [13]. These methods of modeling estimate the relations between the output (response or target variable) and input variables (experimental operating factors) of the process by means of experimentally derived data. Subsequently, derived models are used to approximate the optimum situations of independent variables to minimize or maximize the target variable (dependent variable) [14]. ANNs and RSM have been commonly used to model photocatalytic processes and also optimization interconnected to the degradation of different contaminants for instance pharmaceuticals and dyes[15,16,17] and streams of wastewater such as power plants wastes, dyestuff, etc. [18,19].

To our knowledge, there is no similar study focusing on ANN and RSM modeling techniques for the optimization of COD reduction through photocatalytic reactions in real secondary treated wastewaters of olefin plants.

Taking into account the above discussion, in a batch mode attitude, the effects of factors such as temperature, pH, and catalyst loading on the process of photocatalytic removal of COD in real wastewaters were studied by applying a design of experiment and ANN modeling methods.

2. Experimental

2.1. Material and reagents

In this study, in a normal operational condition, neutralization part outlet of actual spent caustic wastewater of olefin unit has been selected as the inlet wastewater sample into the photocatalytic reactor. The main characteristics of the wastewater sample are given in Table 1.

The main chemicals used in this research were hydrogen peroxide (35 % by volume), sulfuric acid (98 % by weight), and sodium hydroxide (35 % by weight) used to adjust pH. The chemicals used for COD measurements are potassium dichromate, mercury sulfate, silver sulfate, potassium hydrogen phthalate. zinc acetate and ammonia solution are used for preparing ZNO.

Table 1
The main characteristics of actual wastewater used as photocatalytic reactor feed.

Characteristic	Value
COD (ppm)	1280
BOD (ppm)	615
pH	12.5
Phenol(ppm)	25.6
TDS (ppm)	89000
Sulfide(ppm)	7.8

2.2. Synthesis of ZNO photocatalyst

To synthesize the used zinc oxide in this research, precipitation synthesis method was used by using the ultrasonic irradiance. In this method [20], at the environment temperature, 11 grams of zinc acetate were poured into the 100 milliliters of ammonia solution; then, 4 grams of sodium hydroxide were added. Then, the ultrasonic set was filled with the water and connected to the electricity. The

provided solution was carefully placed in the centrifuge set by means of several containers and gained energy for 60 minutes. After that, they were taken out and placed into the centrifuge with 4000 revolutions per minute for 5 minutes to completely precipitate the colloidal nanoparticles; they were separated from the solution. Then, the overhead liquid was emptied; again, nanoparticles were washed by distilled water. Thus, containers were equally filled with the distilled water and, again, were placed in the ultrasonic set till the nano-particles are completely colloidal, and then, they were centrifuged to dissolve the non-nano-particles into the water and, again, the nano-particles were settled. Then, the overhead liquid was emptied and again, the procedure was repeated. Finally, the white color settled particles were placed in the oven for 24 hours at the temperature 60 ^{o}C to be dried gently.

2.2.1. XRD analysis

The structure of synthesized ZnO nanoparticles is specified by XRD analysis in Figure 1. As it can be seen, the peaks of this pattern correspond well with the commercial ZnO and reference pattern peaks (JCPDS Cards 036-1451), indicating the lack of impurity of synthesized compound (index peaks of 100, 002,101, 102, 110, 103, 200, 112, 201, 004). By using the Scherrer formula, the particle size was calculated 40 nanometers.

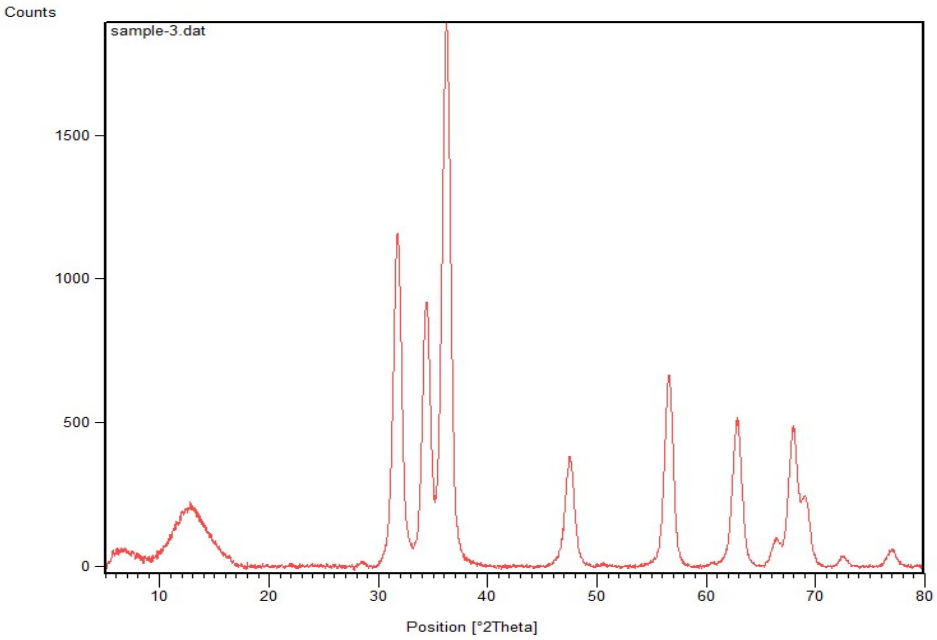

Figure 1. Plot of XRD for synthetic ZnO photocatalyst.

2.2.2. SEM-TEM analysis

As is known, the minimum time for the formation of zinc oxide nanoparticles is 7 minutes in the ultrasonic irradiance; as time increases, the particles' sizes increase orderly. So, with respect to the required particles' sizes, the ultrasonic irradiance time can be adjusted.

The images of the synthesized ZnO nanoparticles are shown in Figures 2 and 3 by using SEM and TEM analyses, respectively. In this image, the dominant pattern for the

geometrical shape of particles is the bar and cauliflower pattern.

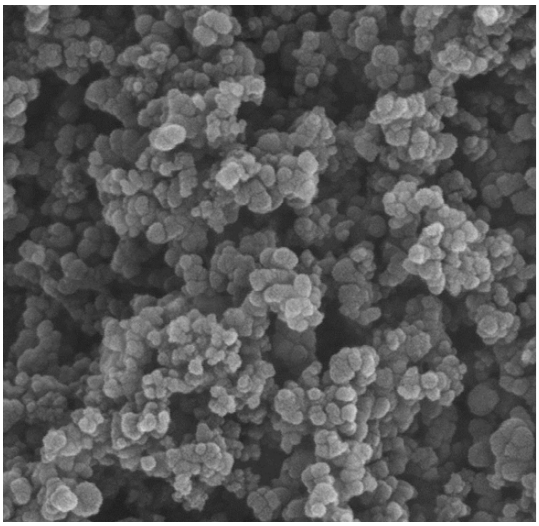

Figure 2. SEM Image of synthetic ZnO photocatalyst.

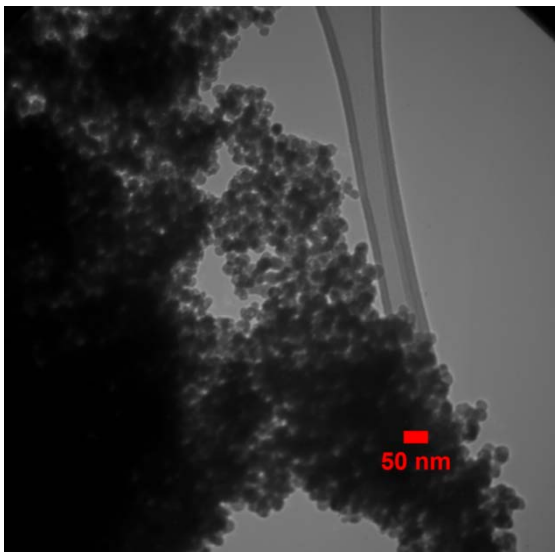

Figure 3. TEM Image of synthetic ZnO photocatalyst.

2.2.3. Determination of the pH of the point of zero charge (pH_{pzc}) in ZNO photocatalyst

At this point, the photocatalyst surface load is neutral through the performance of a test presented by Utrilla, et al. [21], determining the range of adsorption, according to the cationic or anionic nature of the wastewater. This parameter has the value of 8.5 in this research (Figure 4).

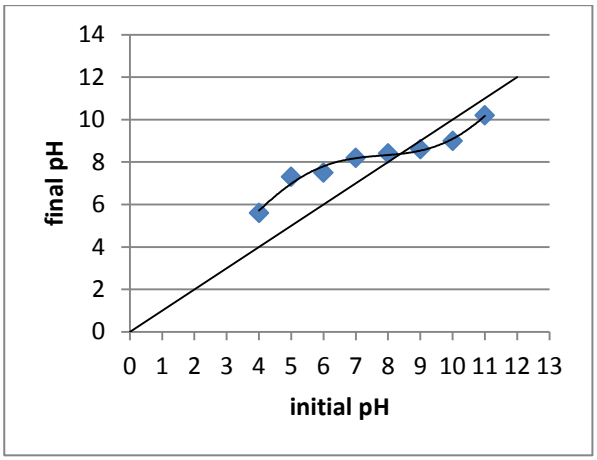

Figure 4. Determination of pH_{pzc} for ZnO photocatalyst.

2.3. Photocatalytic experiments

In this study, the oxidation reactions have been implemented discontinuously in a two-shell photoreactor equipped with an agitator under atmospheric condition. The photocatalyst has been used in the photocatalytic degradation process by dispersing in the solution (slurry state). The slurry reactor is a cylindrical two-shell reactor, made of stainless steel 304. In this reactor, eight 16 W, UV-C lamps were used by means of eight quartz glass sleeves. In order to put lamps into the reactor, 45 × 2 cm quartz tubes were employed in the desired locations. To ensure uniform light throughout the reactor, the distance between lamps must be equal. In order to prevent irradiation to the environment, an aluminum foil was used at the top of the reactor closure during the experiments. Also, Viton gasket was used to barricade the space around quartz glasses after installation. A propeller agitator with three cables propellers was used to mix the reaction solution adjusted with a 12 volts DC

electromotor at 200 revolutions per minute (RPM). The required dissolved oxygen was provided through a compressor of Heila Company with a capacity of 35 l/min. The oxygen passing through a rotameter was injected into the system by an annular aquarium spreader in order to create small bubbles and appropriate air distribution.

The temperature recorded during the whole experiments was in the range 26-28 ºC, indicating almost isothermal conditions. It is evident in photocatalytic reactions in which, in the range of 20 to 80 ºC, temperature does not significantly affect the reaction rate. A schematic diagram of the photocatalytic reactor is shown in Figure 5.

An appropriate amount of catalyst was added to the solution and was riled prior to and also during the irradiation. In order to obtain adsorption steadiness on photocatalyst surface, the mixture was left in the absence of irradiation for 15 minutes before radiance. Equal-volume samples (10 ml) were collected directly from the reactor at the distinct period of time and were filtered to separate ZNO particles before further analytical analysis. By analysing COD reduction percentage after a certain time (90 minutes), the efficiency of the process was examined using the following relation:

$$\% \text{ removal efficiency} = \frac{C_0 - C}{C_0} \times 100 \qquad (1)$$

In this equation, C_0 and C are COD parameters at the beginning of the photocatalytic process (when turning lamps on) and at the end of the process (after 90 minutes).

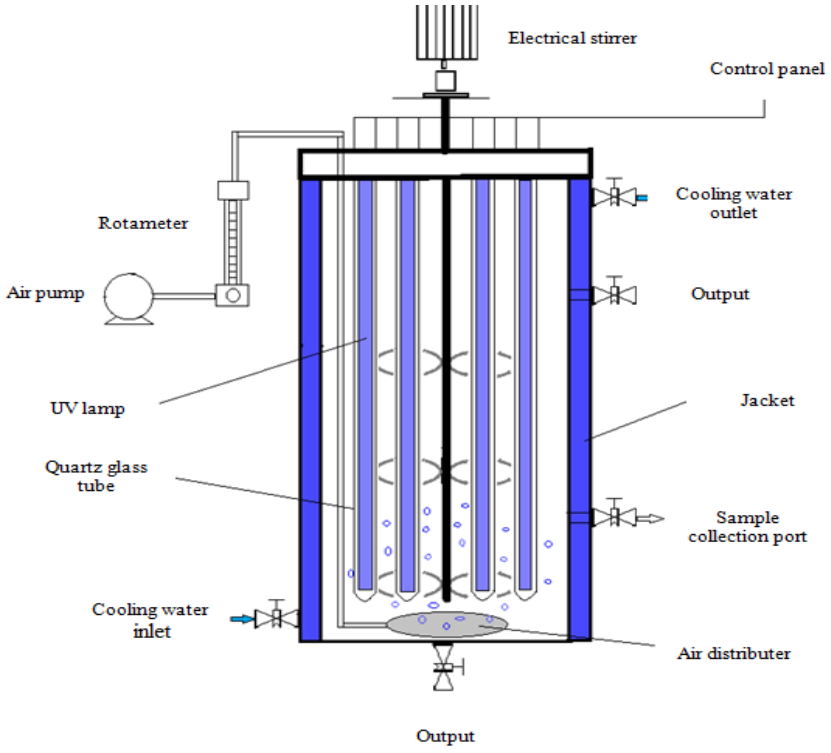

Figure 5. Schematic diagram of the photoreactor.

2.4. Analytical procedures

COD is a major parameter indicating the concentration of wastewater organic compounds. COD shows the equivalent oxygen of oxidized organic compounds by potassium dichromate and silver sulfate under

acidic conditions, which are measured based on APHA standard number 5220. In this study, a spectrometer set model DR5000 was used.

2.5. RSM and ANN modelling

The parameters considered in this study include photocatalyst concentration (A), pH of the initial solution (B), oxidant dosage (C), and aeration rate (D). For optimization of the process variables, some batch tests were conducted according to the Box-Behnken design (BBD). To develop quadratic polynomial models, BBD, a spherical, rotating design, including middle points of the edges of the circle circumscribed on the sphere [22] and few central points are appropriate [23]. Combinations of fewer factors are required and intended to determine the complex response function. Also, it does not have the extreme combinations. According to a four-factor BBD designed in this study, a total number of 30 experiments were carried out. The selected factors with their values are given in Table 2.

Table 2
Variables and their ranges used in this study

Factor	Sign	Code of variables	
		Low	High
		-1	+1
Photocatalyst concentration (g/l)	A	0.5	2
pH	B	4	10
Auxiliary oxidant concentration (ppm)	C	0	300
Aeration rate (l/min^{-1})	D	0.5	4

As is shown in Table 3, the dataset acquired from BBD has been applied to optimize the response of COD photocatalytic degradation. The selection of these factors and their corresponding values was carried out after preliminary experiments which will be described in the results section. The experimental data were then applied in the fitting process using RSM and ANNs.

In response surface modelling, a quadratic polynomial equation was applied to analyze the relation between the target variable and input factors as follows:

$$y = \beta_0 + \sum_{i=1}^{k} \beta_i x_i + \sum_{i=1}^{k} \beta_{ii} x_i^2 + \sum_{1 \le i \le j}^{k} \beta_{ij} x_i x_j + \varepsilon \qquad (2)$$

In the above equation, y represents the target variable of the photocatalytic efficiency, β_0 is a constant, β_{ij}, β_{ii}, β_i are the coefficients of regression for interaction effects, x_i, x_j are independent variables of the process, and ε represents the error [24]. The statistical analysis was performed and a model was suggested. According to the developed model, further analysis was performed through the analysis of variance (ANOVA). The applicability and accurateness of the quadratic model achieved by RSM were determined using the accuracy parameters (R^2, $R^2_{adj.}$). P-values, adequate precision, and F-values (Fisher variation ratio) were determined to analyze the significance of the input variables and the model. The significance of model was evaluated with respect to 95 % confidence level. Finally, three-dimensional plots were depicated to illustrate the effects of interaction terms on COD removal.

Regarding the ANN model, the experimental data were utilized to train the network in the learning process. A typical structure of neural network, which has been

used in this study, is shown in Figure 6. As is shown, the ANN consists of an input layer, a hidden layer, and an output layer. The input variables to the neural network were as follows: catalyst loading (g/l), pH, oxidant dosage (ppm), and aeration rate (l/min). The percentage of COD removal was considered as an experimental output variable.

By changing the hidden layer neurons number (2-20), the optimum number of neurons was derived. Moreover, optimum areas related to the highest photocatalytic removal of COD were determined using the optimal networks. The predicted values were compared with the observed values. As a test for high prediction capability, the verification cases contained in the data set were employed.

Table 3
The four-factor Box-Behnken design matrix with experimental and the results of the two models.

Run	Catalyst loading (g/l)	pH	Oxidant (ppm)	Aeration rate (l/min)	COD removal % (experimental)	COD removal % (ANN)	COD removal% (RSM)
1	1.25	7	150	2.25	73	71	72
2	1.25	7	300	0.5	30	31	34
3	2	10	150	2.25	62	62	63
4	1.25	7	150	2.25	67	71	71
5	2	7	300	2.25	71	71	67
6	0.5	10	150	2.25	15	15	18
7	1.25	10	0	2.25	20	20	15
8	0.5	7	150	0.5	22	23	23
9	1.25	7	300	4	73	73	79
10	0.5	7	0	2.25	12	12	22
11	1.25	4	150	0.5	19	20	24
12	2	7	150	0.5	58	58	50
13	1.25	7	0	0.5	50	49	43
14	1.25	7	0	4	42	42	35
15	1.25	7	150	2.25	71	71	72
16	1.25	7	150	2.25	75	71	72
17	2	7	0	2.25	59	59	68
18	0.5	7	150	4	49	47	42
19	1.25	10	300	2.25	73	73	69
20	1.25	4	0	2.25	61	61	60
21	0.5	4	150	2.25	49	49	46
22	1.25	4	300	2.25	42	42	43
23	1.25	10	150	0.5	31	31	35
24	0.5	7	300	2.25	63	62	60
25	1.25	10	150	4	33	33	33
26	1.25	4	150	4	60	65	62
27	2	7	150	4	64	64	72
28	1.25	7	150	2.25	68	71	69
29	2	4	150	2.25	59	59	54
30	1.25	7	150	2.25	79	71	71

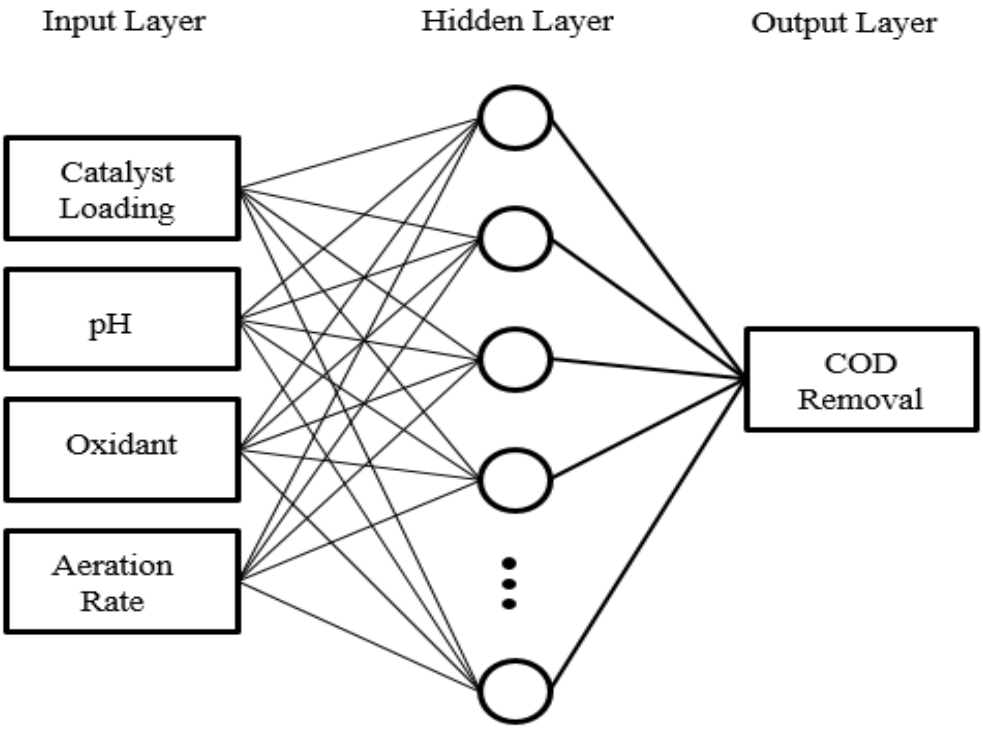

Figure 6. Schematic diagram of the three-layer ANN model with four inputs and one output.

By excluding coefficients of correlation, the adjusted R^2 (R^2_{adj}), R^2, root mean squared error (RMS), absolute average deviation (AAD), and also the mean absolute error (MAE) were applied to examining the used technique. According to Eq. (3), R^2_{adj} was calculated as follows:

$$R^2_{adj.} = 1 - \left[(1 - R^2)\frac{N - 1}{N - K - 1}\right] \qquad (3)$$

where *K* is the sum of independent variables and *N* is the number of all observations [25]. The other characteristics of performance were derived by the following equations:

$$RMS = \frac{\sqrt{\sum_{i=1}^{n}(X_m - X_p)^2}}{n} \qquad (4)$$

$$MAE = \frac{\sum_{i=1}^{n}|X_m - X_p|}{n} \qquad (5)$$

$$AAD = \left\{\frac{\sum_{i=1}^{n}(|X_m - X_p|/X_m)}{n}\right\} \times 100 \qquad (6)$$

In the above equations, X_p and X_m are the target factor values predicted by the model and measured, respectively, and *n* is the sum of data points. The mathematical software of MATLAB 2013b with an ANN toolbox for Windows was employed to study the ANNs topology and make the Single layer perceptrons (SLPs) and surfaces of the response for COD removal. The comparison of RSM and ANNs was made based on R^2, R^2_{adj}, MAE, AAD, and RMS characteristics.

3. Results and discussion

3.1. Factors selection through the preliminary experiments

In order to evaluate the extent of the COD removal, photolysis and adsorption tests were carried out prior to the design of the experimental matrix. Adsorption in the absence of UV illumination and photolysis as

two non-photocatalytic tests was conducted for a distinct time of 90 min. According to the results obtained, the fast degradation rate occurring in the irradiation of mixture containing ZNO cannot be assigned to these two mentioned processes. This fact is clearly evident in Figure 7.

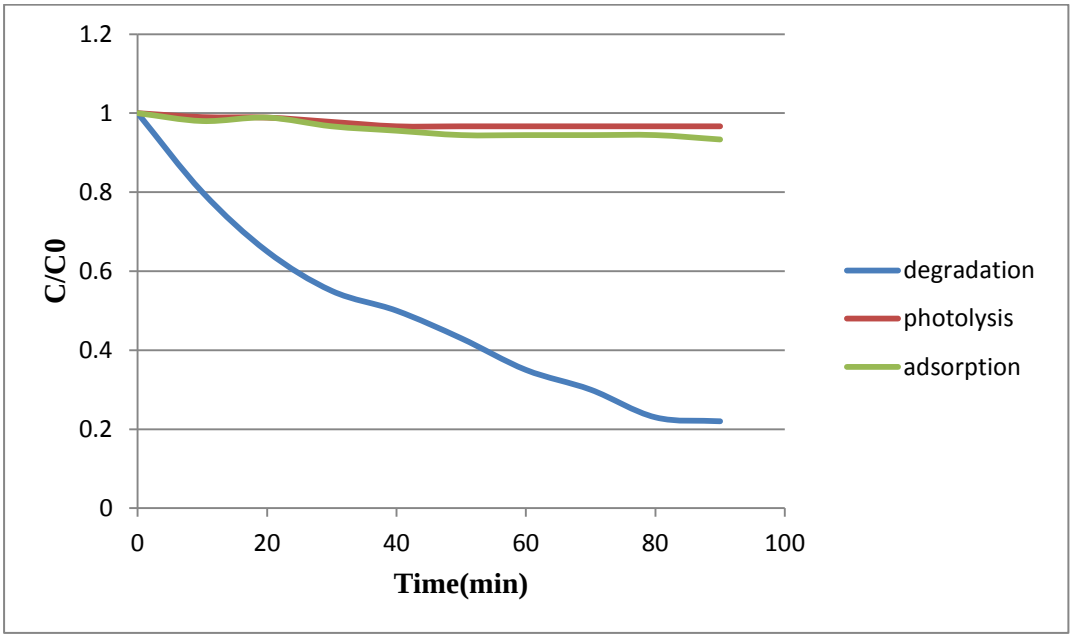

Figure 7. Comparison of the results of absorption and photolysis processes in preliminary tests.

The efficiency of the photocatalytic process depends on a number of factors like pH, UV light strength, catalyst loading, aeration rate, the addition of oxidants, temperature, etc. [26,27]. In this study, a preliminary experiment with 6 factors was performed in order to realize the most important variables based on the fractional factorial design of experiment (Table 4). This design contains 16 experimental runs. The details of the experimental runs are presented in Table 5. According to the analyzed data and with a view of Pareto chart of variables (Figure 8), UV light is the most effective parameter and the temperature is the least effective parameter in the process among the other factors. Therefore, for optimization experiments, UV light was kept constant at its highest level and the temperature was excluded from the investigation. In this way, four factors, including pH, catalyst loading, aeration rate, and oxidant dosage, were considered.

Table 4
Range of various factors used in preliminary tests.

Factor	Sign	Code of variables	
		Low	High
		-1	+1
Temperature (ºC)	A	25	80
Aeration rate (l/min)	B	0.5	3
Catalyst loading (ppm)	C	0.5	2
Light	D	2	8
Oxidant dosage(ppm)	E	0	300
pH	F	4	9

Table 5
Fractional factorial design matrix for screening tests.

Run	A: Temperature (°C)	B: Aeration rate (l/min)	C: Catalyst loading (g/l)	D: Light	E: Oxidant dosage (mg/l)	F: pH	COD removal (%)
1	80.00	3.00	0.50	8.00	0.00	4.00	53
2	25.00	0.50	0.50	8.00	0.00	9.00	30
3	25.00	3.00	0.50	8.00	300.00	4.00	80
4	80.00	0.50	2.00	2.00	0.00	9.00	24
5	80.00	3.00	0.50	2.00	0.00	9.00	12
6	80.00	0.50	0.50	8.00	300.00	9.00	50
7	25.00	0.50	2.00	8.00	300.00	4.00	91
8	80.00	0.50	0.50	2.00	300.00	4.00	37
9	25.00	3.00	0.50	2.00	300.00	9.00	29
10	25.00	0.50	0.50	2.00	0.00	4.00	17
11	25.00	3.00	2.00	2.00	0.00	4.00	45
12	80.00	0.50	2.00	8.00	0.00	4.00	65
13	80.00	3.00	2.00	8.00	300.00	9.00	86
14	25.00	3.00	2.00	8.00	0.00	9.00	66
15	25.00	0.50	2.00	2.00	300.00	9.00	41
16	80.00	3.00	2.00	2.00	300.00	4.00	64

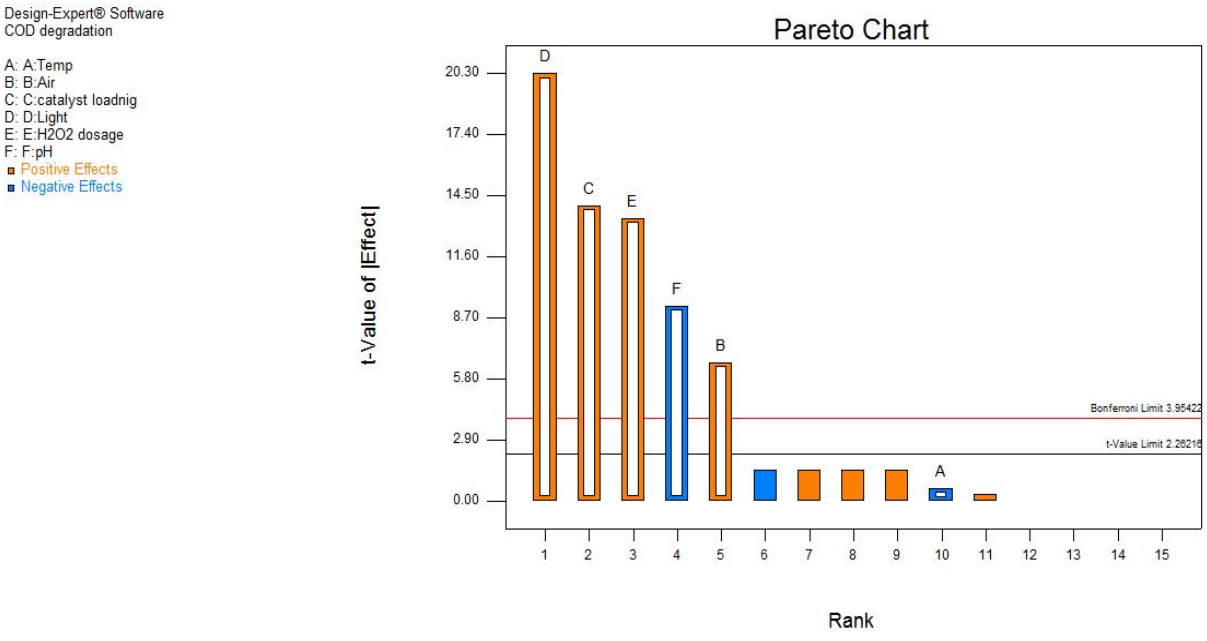

Figure 8. Pareto chart depicting the ranks of factors.

3.2. Modelling and optimization based on RSM

A BBD matrix with four factors and the results of experimental runs in term of photocatalytic removal percentage are shown in Table 3. According to the considered experimental design, a second-order model was derived experimentally for fitting data.

This model is represented by the following coded equation:

$$\%\ \text{COD removal} = +71.83 + 13.51A - 4.71B + 9.00C + 9.12D + 9.16AB - 9.81AC - 9.82BD + 17.89BC + 12.75CD - 9.58A^2 - 17.04B^2 - 7.99C^2 - 16.19D^2 \quad (7)$$

The model accuracy is demonstrated in Figure 9 through the comparison between the actual values and predicted ones. The results show the good accuracy of the model. Moreover, the low value of the coefficient of variation (CV = 3.88 %) confirms the good accuracy of the model. The model significance and adequacy have been examined by means of ANOVA (Table 6). Statistical values, including p-value <0.0001 and F-value of 18.87, reveal the model's high significance. There is only a chance of 0.01 % that F-value of the model could happen because of error. Also, good model's predictability can be approved by the lack of fit test (not significant in this case) corresponding to the absolute error. Considering R^2 of 0.9388, the variability of 93.88 % could be described sufficiently via the obtained results; accordingly, the overall variation of 0.73 % remained inexplicable. The adjusted coefficient value of 0.8890 and its reasonable consistence with R^2 reveal good predictability of the model. Furthermore, the analysis of residuals was performed to evaluate the model adequacy. Figure 10 illustrates normal probability of studentized residuals. This figure is interesting to discover whether the error variation is uniform. The points near the diagonal line confirm that there is no significant deviation of non-normality, uniform error variances, and independence of the residuals. The overall results indicated the adequacy of the model to explain the process in the range of operating conditions studied.

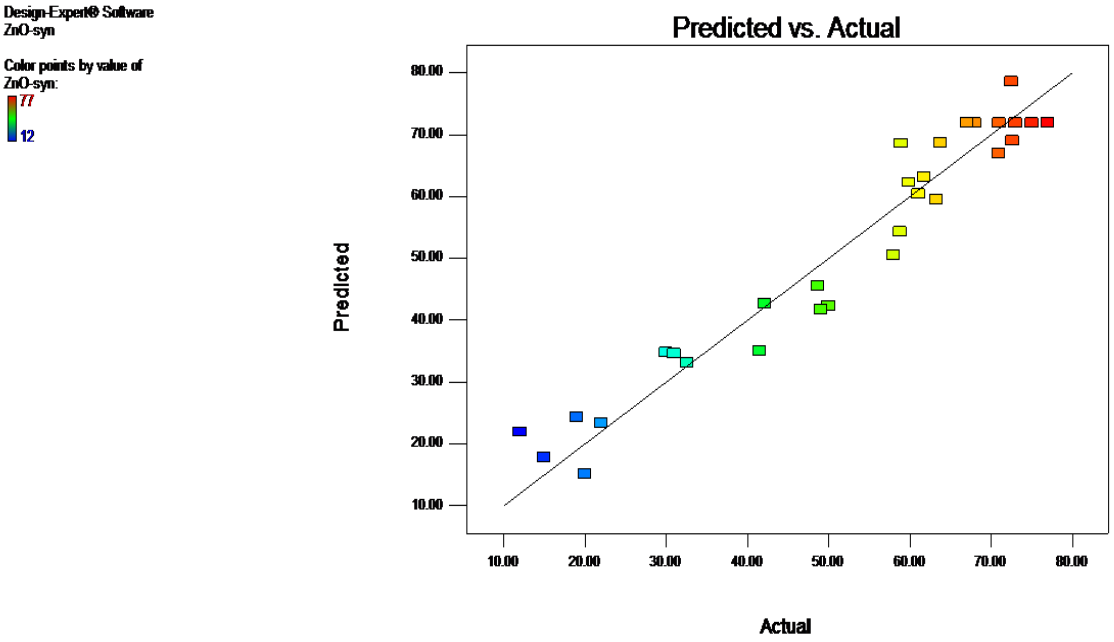

Figure 9. Experimental data versus predicted data obtained from RSM.

Table 6
Analysis of variance in response surface model.

Source	Sum of squares	df	Mean square	F-value	p-value prob>F
Model	11062.26	13	850.94	18.87	<0.0001significant
A- Catalyst loading	2188.90	1	2188.90	48.54	<0.0001
B- pH	266.60	1	266.60	5.91	0.0272
C- C_{H2O2}	971.70	1	971.70	21.55	<0.0003
D- Air	997.25	1	997.25	22.11	<0.0002
AB	335.40	1	335.40	7.44	<0.0149
AC	385.22	1	385.22	8.54	<0.0100
CD	650.26	1	650.26	14.42	<0.0001
BC	1280.79	1	1280.79	28.40	<0.0001
BD	385.84	1	385.84	8.56	<0.0001
A^2	629.69	1	629.69	13.96	0.0018
B^2	1991.73	1	1991.73	44.17	<0.0001
C^2	437.26	1	437.26	9.70	<0.0067
D^2	1796.76	1	1796.76	39.84	<0.0001
Residual	721.54	16	45.10	-	-
Lack of fit	644.70	11	58.61	3.81	0.0755 non-significant
Pure error	76.83	5	15.37	-	-
Cor total	11783.80	29	-	-	-

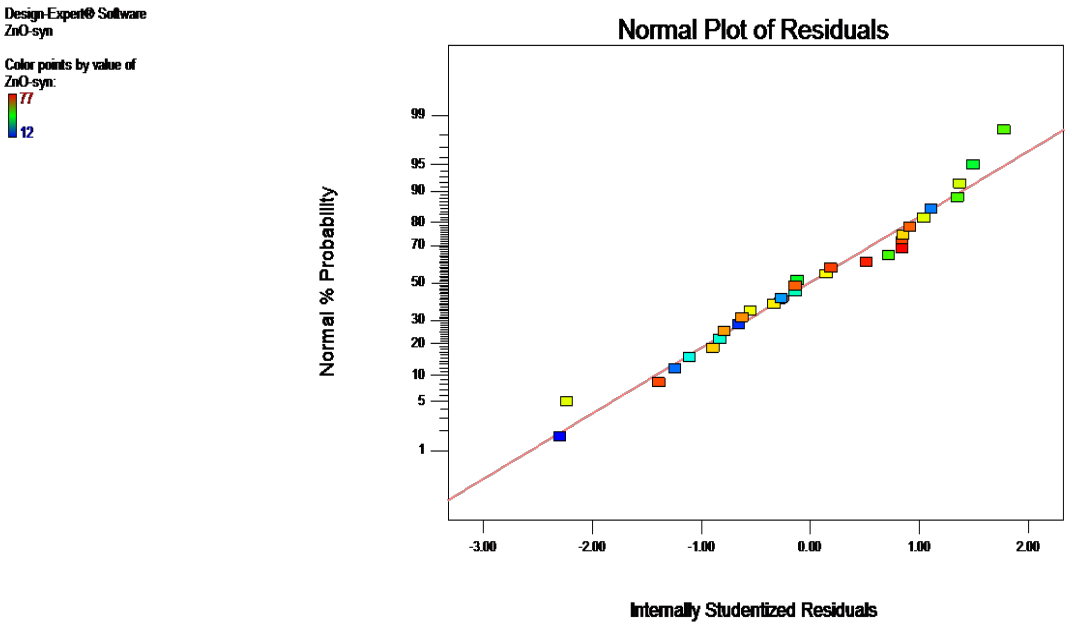

Figure 10. The normal probability diagram of the experimental data.

The significance of all model's terms was assessed by p-values considering 5 % level of significance. The smaller p-value indicates the higher significance of the related terms [28]. The terms of the model, including catalyst loading (A), pH (B), oxidant dosage (C), aeration rate (D), the quadratic effects, and most of the interactions between individual factors, are significantly important factors since $p < 0.001$. The model is based on a second-order polynomial equation the non-significantly important terms of which (p -value >0.05) have been omitted based on a backward elimination method. According to the results, the AD term (Catalyst Loading-aerating rate interaction) has been omitted as it is nonsignificant.

In the polynomial equation, the coefficients indicate the power of each factor (A, B, C, and D) in addition to the interaction terms, the second-order coefficients, and the cross-product coefficients. According to the coefficient quantities in the predictive model, the effect of all terms was calculated using Eq. (8):

$$\% P_i = \frac{b_i^2}{\sum b_i^2} \qquad (8)$$

where P is the efficacy percent of each term and b is the coefficient of each term of the model (according to Eq. (7)). Considering this equation, the effect of each parameter is illustrated in Figure 11. In this figure, blue bars indicate terms with positive effects on the model, and red bars show terms with negative effects. As is observed, all factors, except pH, have positive effects on the model. In other words, if the interaction effects are not considered, as each of factors (except pH) increases, COD removal percent will increase. The interaction term of catalyst loading and pH (AB), the interaction term of pH and oxidant dosage (BC), the interaction term of oxidant dosage and aeration rate (CD) have positive effects; the interaction term of catalyst loading and oxidant dosage (AC) as well as interaction term of pH and aeration rate (BD) have negatively affected the model.

The negative second-order terms were attained for all the factors studied that correspond to concave surfaces, showing a higher rate of decrease of COD removal efficiency at the very high level of the main factors over the considered range of experiments.

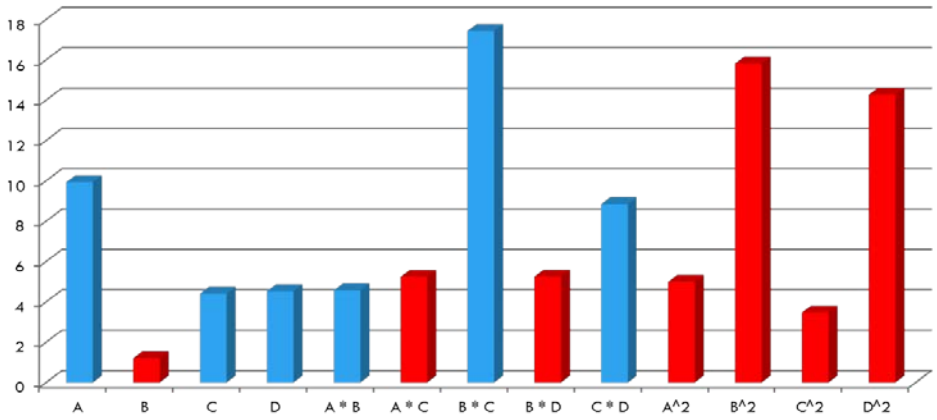

Figure 11. Contribution percent of each term in model obtained by Eq. (7).

Three-dimensional plots of Figure 12 and contour plot of Figure 13 show the effective interactions between pH of initial solution and catalyst loading at three different levels of

auxiliary oxidizer amount and a middle level of aeration rate. Saddle shape shows the interaction effects of two parameters. The production rate of hydroxyl radical increases at the acidic pH. Besides, at the acidic pH, photocatalyst particles have a high tendency towards agglomeration. Thus, when photocatalyst concentration increases, photocatalyst rapidly agglomerates and, with reducing capability of effective absorption and pollutant, degradation reaction rate decreases due to the reduction of positive electron hole and the obtained oxidizer radicals. Therefore, at low concentration of photocatalyst, the acidic pH is more suitable.

At higher concentrations of the photocatalyst, higher pH values are required to prevent agglomeration. However, hydroxyl radical production is only probable with a reaction of a positive hole and water molecule or hydroxide ion. Since the number of photocatalyst increase, lack of the second source of hydroxyl radical (hydroperoxyl radical) production retrieves. At alkaline pH values, due to the negative charge on the sources of the both photocatalysts, pollutant absorption and, consequently, the degradation rate decrease.

Preventing recombination of electron-hole pairs using auxiliary oxidizer is an effective way to increase the efficiency of photocatalytic degradation. Oxygen is commonly used as an electron catcher, and the use of an oxidizer agent (electron absorbent) can increase photocatalytic degradation rate through one of the following reasons [29].

- Electron absorption prevents recombination of electron/hole.
- It increases hydroxyl radical production or other oxidizers in the solution.

The higher amount of oxidizer leads to an increase in the adsorption rate. Since photocatalytic processes have higher efficiency at low pH, the existence of oxidizer at high level prevents the negative effect of high pH values. In other words, pH and oxidizer have positive interaction effect on the process. In addition, when the oxidizer is at its low level, as pH value increases, the removal efficiency decreases.

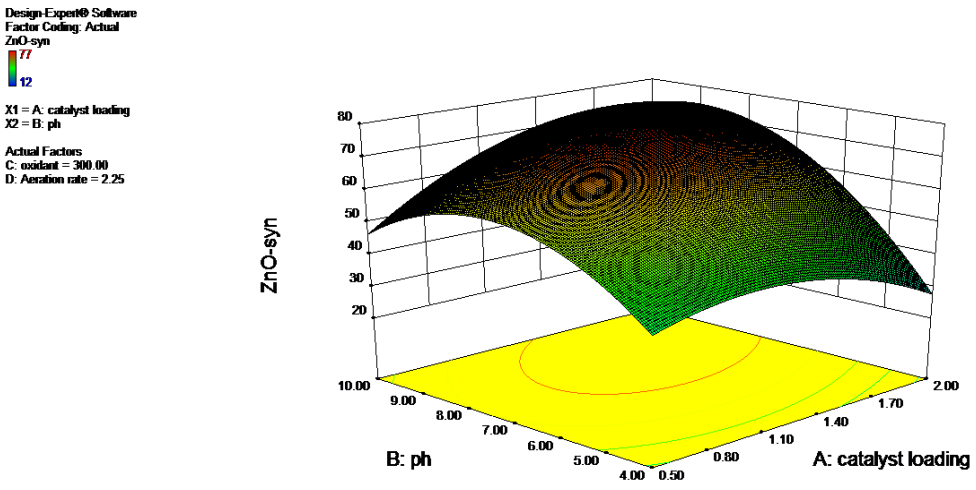

(a)

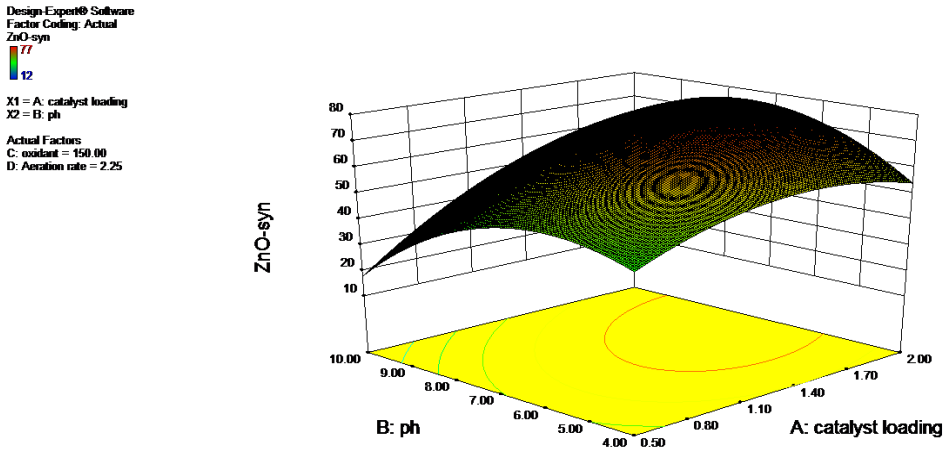

(b)

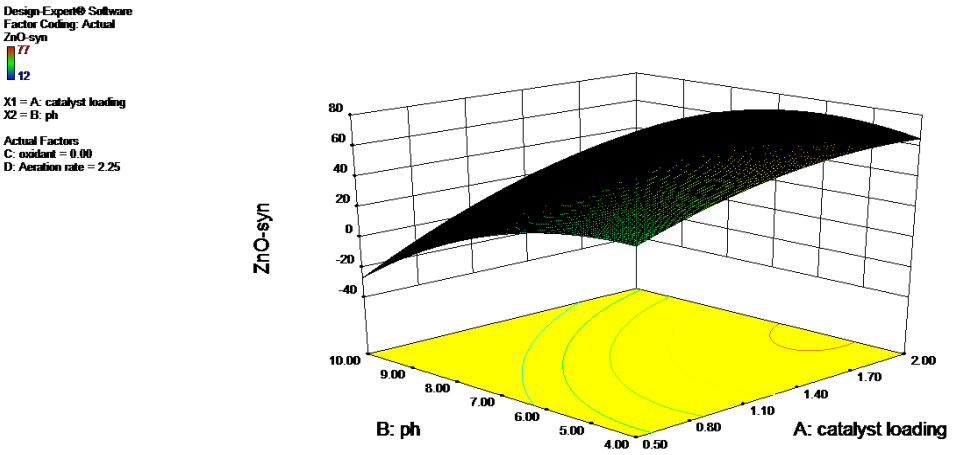

(c)

Figure 12. Three-dimensional plots of changes of photocatalyst loading, pH at various amounts of oxidant dosage and mediocre amounts of aeration obtained from RSM model: (a) maximum amount of oxidant (300 ppm), (b) medium amount of oxidant (150 ppm), and (c) minimum amount of oxidant (0 ppm).

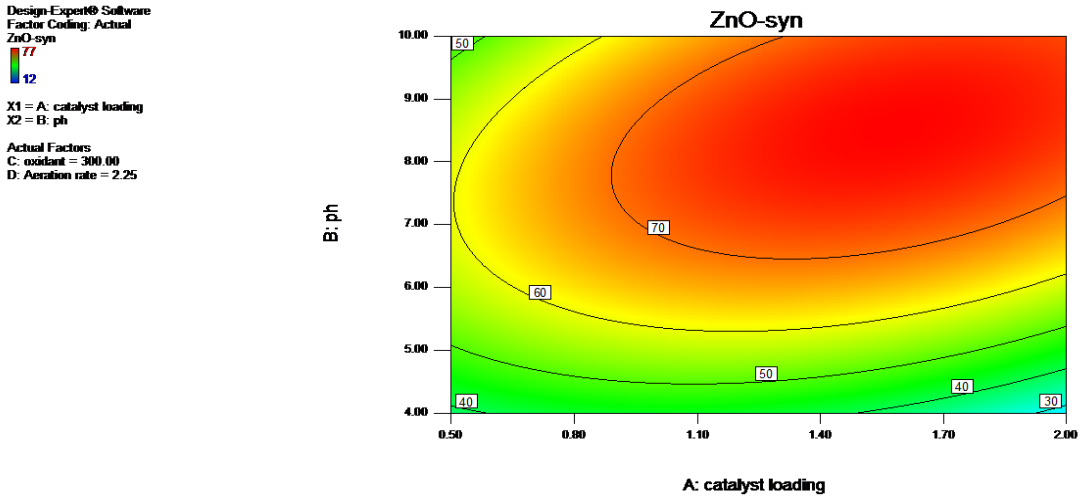

(a)

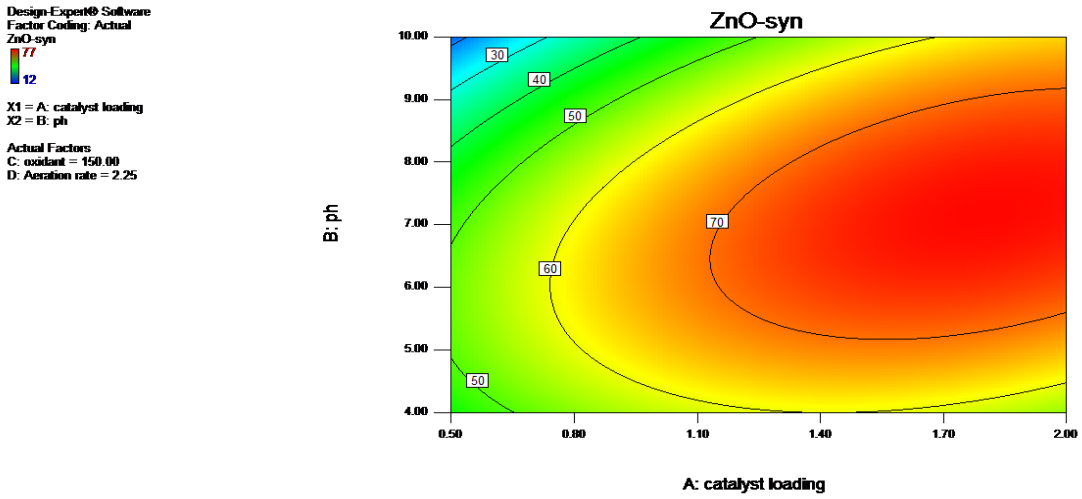

(b)

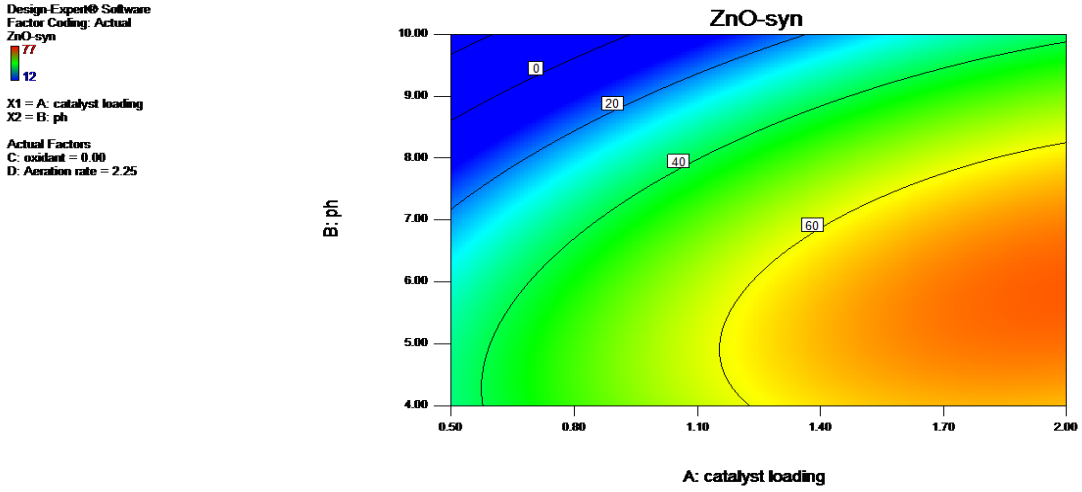

(c)

Figure 13. Contour plots of changes of photocatalyst loading, pH at various amounts of oxidant dosage and a medium amount of aeration obtained from RSM model: (a) maximum amount of oxidant (300 ppm), (b) medium amount of oxidant (150 ppm), and (c) minimum amount of oxidant (0 ppm).

The numerical optimization procedure was performed by applying desirability approach to discovering the distinct settings which give the maximize removal of COD. The details of parameter settings for optimization are presented in Table 7. The maximum COD removal efficiency (~80 %) was achieved in optimum conditions as follows: Catalyst Loading=1.29 g/l, pH 7.08, oxidant dosage=253.66 ppm, and aeration rate=3.17 l/min.

Table 7
Optimum conditions of the COD removal obtained.

Upper Limit	Lower Limit	Goal	Name
A: Catalyst loading (g/l)	is in range	0.5	2
B: pH	is in range	4	10
C: Oxidant dosage (ppm)	is in range	0	300
D: Aeration rate (l/min)	is in range	0.5	4
% COD removal	maximize	12	77

3.3. Modelling and optimization based on ANN

The ANN-based process model was developed by means of the SLP architecture. The SLP network has four input nodes indicating the four input factors, namely catalyst loading, pH, oxidant dosage and aeration rate, and single output node, representing the COD removal determined in batch experiments.

The network was trained through feedforward of input training pattern. In the feed-forward neural net, all neurons of a particular layer are connected to all neurons in its neighborhood. Trainbr is a network training function that updates the weight and bias values according to Levenberg-Marquardt optimization. It minimizes a combination of squared errors and weights and, then, determines the correct combination so as to produce a network that generalizes well. The process is called Bayesian regularization. The training parameters and the range of data used as input and output variables of ANN are listed in Tables 8 and 3, respectively.

Table 8
ANN training parameters.

Parameter	Value
Number of input nodes	4
Number of hidden neurons	6
Number of output node	1
Learning rule	Bayesian Regularization
Number of epochs	1000
Hidden layer transfer function	tansig
Output layer transfer function	purely
μ (Speed of training)	0.005

In this study, different numbers of neurons from 2 to 20 were tested in the hidden layer. The optimum number of neurons was determined based on correlation coefficient and the minimum value of MSE of overall data (Figure 14). Three runs were performed for each network structure using different random values of initial weights.

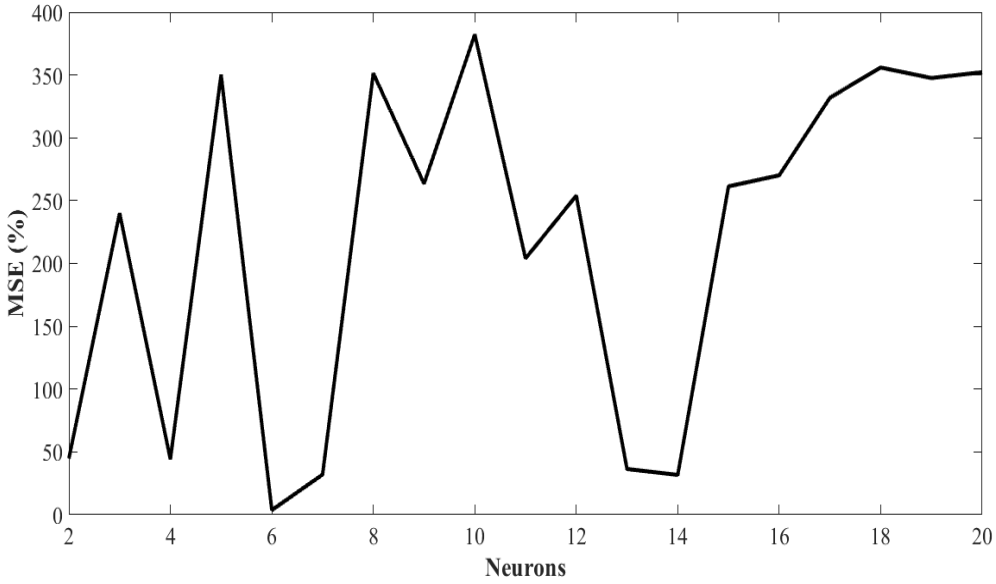

Figure 14. The relationship between number of neurons and MSE.

The experimental and predicted results are summarized in Table 3. The total number of the dataset was 30, whereas 24 datasets were used to train the network; the remaining six data were used for its validation. Moreover, the use of random data (6 points of dataset) as test dataset proved the accuracy of prediction data from the network. The results of comparison between prediction data and test data indicated they were significant with high accuracy of more than 95 percent. The results of fitting with whole data are presented in Figure 15. As is seen, the ANN model provides accurate predictions in the training of ANN. The trend of COD removal percent predicted by the ANN completely follows the observed trend with a high value of R2 (R2 = 0.9904). A high value of R2 near to 1 associated with the low and comparable MAE value and RMS showed that the ANN model suggests excellent generalization characteristics and suitable approximation. Therefore, the ANN model is appropriate for predicting and simulating the COD removal.

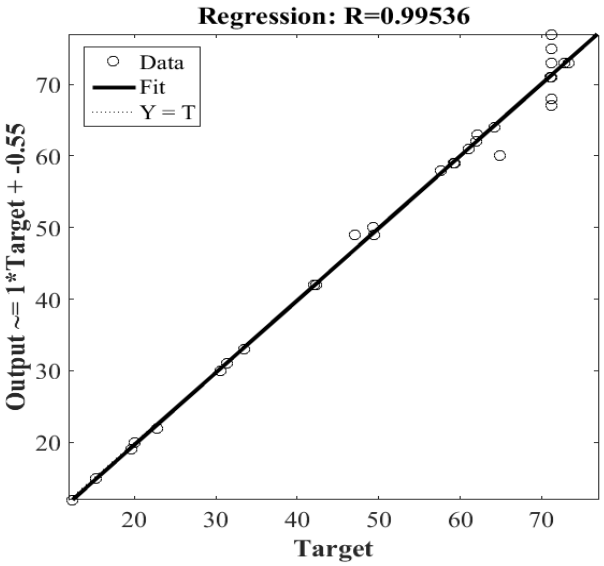

Figure 15. Comparison between experimental and predicted results of the ANN model.

To obtain surfaces plots of response within the whole range of experiments, the optimized ANN was applied. The impact of factors on the COD removal efficiency and the optimization was considered through the values of target variable (Figure 16). The optimum conditions for the maximum COD removal were determined using three-dimensional plots. The results showed that the obtained optimum conditions were similar to those conditions achieved in response surface model. In the optimized conditions, further experiments were conducted that verified the model validity and suitability for simulating the COD removal performance.

3.4. Comparative study on ANN and RSM models

The estimations of the RSM and ANN models are compared with each other in Table 9, consisting of statistical values including correlation coefficients, AAD, RMS, and MAE in the both approaches. In a good model, R^2 should be close to 1.0 and also in good agreement with R^2_{adj}. RMS should be close to zero, and AAD between the observed and predicted values must be as small as possible, while higher values of AAD and RMS imply larger deviations in estimation. As is observed, large values of R^2, R^2_{adj} as well as small difference between them in the both ANN and RSM indicate the accuracy of the models. In contrast, magnitudes of RMS and AAD in the RSM were more than those of RMS and AAD in ANN. Though both ANN and RSM models suggested suitable estimation efficiency, the ANN approach showed better predictions in comparison with RSM.

The response surface model is limited to a quadratic polynomial equation. ANN provides a more genuine method of modelling in comparison with RSM, since it estimates the system curvature much better. Also, ANN

is suitable for optimizing multivariate processes, while RSM model should be run more than a few times [30].

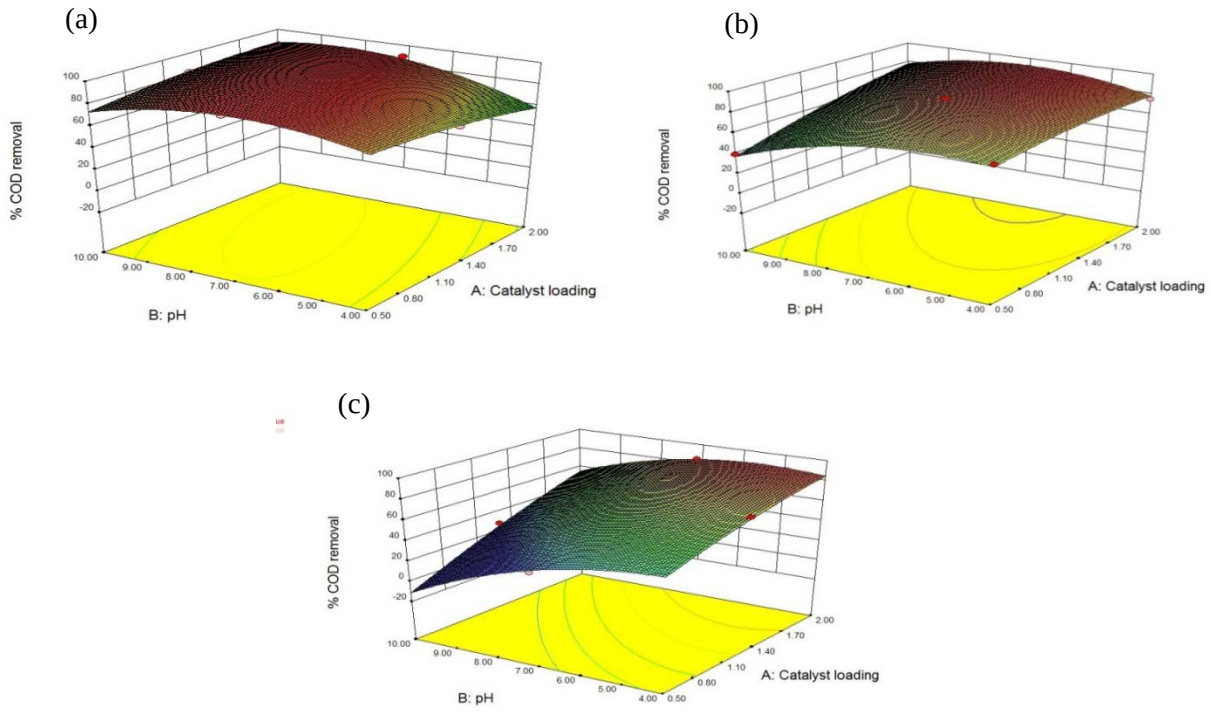

Figure 16. Three-dimensional plots of parameters changes of photocatalyst loading, pH at various amounts of oxidant dosage and mediocre amount of aeration(For ANN model): a) Maximum amount of oxidant(=300 ppm), b) A mediocre amount of oxidant (=150), and c) Minimum amount of oxidant (=0 ppm).

Table 9
Comparison of prediction and optimization results of ANN and RSM.

Parameters	RSM	ANN
R^2	0.9388	0.9904
R^2_{adj}	0.8890	0.9973
RMS	0.6408	0.2115
MAE	0.502	0.2106
AAD	0.7662	0.3453

4. Conclusions

ANN and RSM were employed to model and optimize the photocatalytic removal of COD in aqueous suspension including ZNO. A BBD was successfully applied to assess the effect of catalyst loading, oxidant dosage, pH and aeration rate on the photocatalytic degradation performance, verifying that the all factors investigated had considerable influences. By means of RSM and ANN, the experimentally derived data were fitted. Moreover, optimum values were found during the use of these methods. By using R^2 values, MAE, RMS and AAD, the accuracy of the both models were examined and compared. The obtained results evidenced that the ANN model showed higher accuracy than the response surface model did. The results represent the capability of the trained artificial neuron networks for assessing the non-linear behavior of the system.

References

[1] Wang, G. S., Liau, H., Chen, H. W. and Yang, H. C., "Characteristics of natural organic matter degradation in water by UV/ H_2O_2 treatment", *Environmental Technology*, **27**, 277 (2006).

[2] Ellis, C. E., "Wet air oxidation of refinery spent caustic", *Environmental*

Progress, **17** (1), 28 (2000).

[3] Tania Mara, S. and Carlos, "Wet air oxidation of refinery spent caustic: A refinery case study", *NPRA Conference*, San Antonio, Texas, (2000).

[4] Sheu, S. H. and Weng, H. S., "Treatment of olefin plant spent caustic by combination of neutralization and fenton reaction", *Water Research*, **35** (8), 2017 (2001).

[5] Rodriguez, N., Hansen, H. K., Nunez, P. and Guzman, J., "Spent caustic oxidation using electro-generated Fenton's reagent in a batch reactor", *Journal of Environmental Science and Health, Part A*, **43** (8), 952 (2008).

[6] Nunez, P., Hansen, H. K., Rodriguez, N., Guzman, J. and Gutierrez, C., "Electrochemical generation of Fenton's reagent to treat spent caustic wastewater", *Separation Science and Technology*, **44** (10), 2223 (2008).

[7] Yu, Z. Z., Sun, D. Z., Li, C. H., Shi, P. F., Duan, X. D., Sun, G. R. and Liu, J. X., "UV-catalytic treatment of spent caustic from ethane plant with hydrogen peroxide and ozone oxidation", *Journal of Environmental Science*, **16** (2), 272 (2004).

[8] Hawari, A., Ramadan, H., Abu-Reesh, I. and Ouederni, M., "A comparative study of the treatment of ethylene plant spent caustic by neutralization and classical and advanced oxidation", *Journal of Environmental Management*, **151**, 105 (2015).

[9] Abdulah, S. S., Hassan, M. A., Noor, Z. Z. and Aris, A., "Optimization of photo-fenton oxidation of sulfidic spent caustic by using response surface methodology", *Journal of Environmental Science*, **25** (4), 231 (2011).

[10] Chen, C., "Wet air oxidation and catalytic wet air oxidation for refinery spent caustic degradation", *J. Chem. Soc. Pak.*, **35** (2), 121 (2013).

[11] Alaiezadeh, M., "Spent caustic wastewater treatment with electrical coagulation method", *The 1st International Conference Oil, Gas, Petrochemical and Power Plant*, (2015).

[12] Montgomery, D. C., "Design and analysis of experiments", 6th Edition, John Wiley & Sons, (2013).

[13] Behjoomanesh, M., Keyhani, M., Ganji-Azad, E., Izadmehr, M. and Riahi, S., "Assessment of total oil production in gas-lift process of wells using Box–Behnken design of experiments in comparison with traditional approach", *Journal of Natural Gas Science and Engineering*, 27, 1455 (2015).

[14] Fox, R. J., Elgart, D. and Davis, S. C., "Bayesian credible intervals for response surface optima", *Journal of Statistical Planning and Inference*, **139**, 2498 (2009).

[15] Khataee, A. R. and Kasiri, M. B., "Artificial neural networks modeling of contaminated water treatment processes by homogeneous and heterogeneous nanocatalysis", *J. Mol. Catal., A: Chem.*, **331**, 86 (2010).

[16] Sakkas, V. A., Calza, P., Medana, C., Villioti, A. E., Baiocchi, C., Pelizzetti, E. and Albanis, T., "Heterogeneous photocatalytic degradation of the pharmaceutical agent salbutamol in aqueous titanium dioxide suspensions", *Applied Catalysis, B: Environmental*, **77**, 135 (2007).

[17] Sleiman, M., Vildozo, D., Ferronato, C.

and Chovelon, J. M., "Photocatalytic degradation of azo dye Metanil Yellow: Optimization and kinetic modeling using a chemometric approach", *Applied Catalysis, B: Environmental*, **77**, 1 (2007).

[18] Secula, M. S., Suditu, G. D., Poulios, I., Cojocaru, C. and Cretescu, I., "Response surface optimization of the photocatalytic decolorization of a simulated dyestuff effluent", *Chem. Eng. J.*, **141**, 18 (2008).

[19] Keramati, N., Nasernejad, B. and Fallah, N., "Photocatalytic degradation of styrene in aqueous solution: Central composite design optimization", *JDST*, **35**, 1543 (2014).

[20] Zak, A. K., Wang, H. Z., Yousefi, R., Golsheikh, A. M. and Ren, Z. F., "Sonochemical synthesis of hierarchical ZnO nanostructures", *Ultrasonics sonochemistry*, **20** (1), 395 (2013).

[21] Rivera-Utrilla, J., Bautista-Toledo, I., Ferro-García, M. A. and Moreno-Castilla, C., "Activated carbon surface modifications by adsorption of bacteria and their effect on aqueous lead adsorption", *Journal of Chemical Technology and Biotechnology*, **76**, 1209 (2001).

[22] Evans, M., Optimisation of manufacturing processes: A response surface approach, Maney Pub., (2003).

[23] Nazzal, S. and Khan, M. A., "Response surface methodology for the optimization of ubiquinone self-nano emulsified drug delivery system", *AAPS Pharm Sci. Tech.*, **3**, 23 (2002).

[24] Ranjan, D., Mishra, D. and Hasan, S. H., "Bioadsorption of arsenic: An artificial neural networks and response surface methodological approach", *Ind. Eng. Chem. Res.*, **50**, 9852 (2011).

[25] Nelofer, R., Ramanan, R. N., Rahman, R. N. Z. R. A., Basri, M. and Ariff, A. B., "Comparison of the estimation capabilities of response surface methodology and artificial neural network for the optimization of recombinant lipase production by E. coli BL21", *Journal of Ind. Microbiol. Biotechnol.*, **39**, 243 (2012).

[26] Konstantinou, I. K. and Albanis, T. A., "Photocatalytic transformation of pesticides in aqueous titanium dioxide suspensions using artificial and solar light: Intermediates and degradation pathways", *Applied Catalysis, B: Environmental*, **42**, 319 (2003).

[27] Konstantinou, I. K. and Albanis, T. A., "TiO_2-assisted photocatalytic degradation of azo dyes in aqueous solution: kinetic and mechanistic investigations: A review", *Applied Catalysis, B: Environmental*, **49**, 1 (2004).

[28] Antonopoulou, M. and Konstantinou, I., "Photocatalytic degradation of pentachlorophenol by visible light N-F-TiO_2 in the presence of oxalate ions: Optimization, modeling and scavenging studies", *Environmental Science and Pollution Research*, **22**, 9438 (2015).

[29] Aisien, F. A., Amenaghawon, N. A. and Ekpenisi, E. F., "Photocatalytic decolourisation of industrial wastewater from a soft drink company", *JEAS*, **9**, 11 (2013).

[30] Ranjan, D., Mishra, D. and Hasan, S. H., "Bioadsorption of arsenic: An artificial neural networks and response surface methodological approach", *Ind. Eng. Chem. Res.*, **50**, 9852 (2011).